Journal of Alloys and Compounds. Vol. 395. Núm. 1-2. 2005. Pag. 313-317
http://dx.doi.org/10.1016/j.jallcom.2004.11.057

Effect of Partial Substitution of Ge for B on the High Temperature Response of Soft Magnetic Nanocrystalline Alloys

J. S. Blázquez,[1,2] S. Roth,[1] A. Conde [2]

[1] *IFW-Dresden, Institute for Metallic Materials, Helmholtzstrasse 20, 01069 Dresden, Germany.*

[2] *Departamento de Física de la Materia Condensada. ICMSE-CSIC. Universidad de Sevilla. P.O. Box 1065. 41080 Sevilla, Spain.*

Abstract

The effect of partial substitution of Ge for B in $Fe_{78}Co_5Zr_6B_{10}Cu_1$ alloy on the microstructure, crystallization process and magnetic properties of the amorphous and nanocrystalline alloys was studied. Special attention was focused on the saturation magnetization response at high temperature and its dependence on the microstructure. Although the Curie temperature of the amorphous phase is not affected by the partial substitution of Ge for B, the saturation magnetization increases ~10 % with respect to the alloy without Ge.

Keywords: A nanostructures, D magnetic measurements

*Corresponding author: S. Roth

IFW-Dresden, Institute for Metallic Materials

Helmholtzstrasse 20, 01069 Dresden, Germany.

Phone: (+49) (0) 351 4659 2 49

Fax: (+49) (0) 351 4659 541

E-mail: s.roth@ifw-dresden.de

Journal of Alloys and Compounds. Vol. 395. Núm. 1-2. 2005. Pag. 313-317
http://dx.doi.org/10.1016/j.jallcom.2004.11.057

1. Introduction

Nanocrystalline alloys produced by partial devitrification of Fe-B-(Si) amorphous alloys with small addition of Nb, Zr or Hf and Cu are among the softest magnetic materials known up to date [1]. The presence of B facilitates the amorphization of the melted composition by rapid quenching techniques. The ultra-soft magnetic properties of these alloys are due to their particular microstructure, in which nanocrystals of ferromagnetic α-Fe type phase (~10 nm in size) are embedded in a residual amorphous matrix, also ferromagnetic but with a lower Curie temperature. The ferromagnetic character of this matrix enables the exchange coupling between nanocrystals, which yield a severe reduction of the magnetocrystalline anisotropy [2].

As the nanocrystals become uncoupled above the Curie temperature of the residual amorphous phase, T_C^{am}, [3] this parameter is very important to determine the viability of high temperature applications of nanocrystalline compositions. Partial Co substitution for Fe in HITPERM alloys produces a clear increase of T_C^{am} [4]. Unfortunately, soft magnetic properties are impoverished due to the high value of the magnetostriction constant of the α'-Fe,Co crystalline phase developed [5,6], although high saturation magnetization and a wide thermal regime of constant permeability were achieved [7]. Recently, Suzuki et al. proposed the partial substitution of Ge for Fe to enhance the high temperature applications of NANOPERM alloys and concluded that this substitution is more effective than Co substitution for Fe [8]. However, the substitution of Fe for a "non-magnetic" atom provokes a reduction of the magnetization of the material.

In this work, the effects of partial substitution of Ge for B on the microstructure and the magnetic properties of $Fe_{78}Co_5Zr_6Cu_1B_{10}$ and $Fe_{78}Co_5Zr_6Cu_1B_5Ge_5$ alloys are studied. The Co addition was chosen low enough to avoid a deleterious effect on the magnetostriction of the crystalline phase [9], keeping the magnetoelastic anisotropy of the whole system at low values.

Journal of Alloys and Compounds. Vol. 395. Núm. 1-2. 2005. Pag. 313-317
http://dx.doi.org/10.1016/j.jallcom.2004.11.057
On the other hand, this small addition of Co will increase the Curie temperature, as well as the magnetization, of both phases in the nanocrystalline system.

2. Experimental techniques

Ribbons (5 mm wide and 20-30 μm thick) of $Fe_{78}Co_5Zr_6B_{10}Cu_1$ and $Fe_{78}Co_5Zr_6Ge_5B_5Cu_1$ compositions were obtained in amorphous structure by melt-spinning. The crystallization process was studied by differential scanning calorimetry (DSC) using a Netzsch DSC-404C calorimeter. The microstructure was characterized by X-ray diffraction (XRD) using Co-Kα radiation. The magnetic properties were studied in terms of saturation magnetization (M_S) and Curie temperature (T_C), using a Faraday magnetometer, and coercivity (H_C), using a hysteresis loop tracer on long samples (length ~150 mm).

3. Results and discussion

3.1 Devitrification process

Figure 1 shows the DSC scans performed at 10 K/min for as-cast samples of both studied alloys. The devitrification occurs in two different stages. The first broad exothermic peak corresponds to the development of the nanocrystalline microstructure and, after the second crystallization event, intermetallic phases as Fe_2Zr appear deteriorating the magnetic properties of the system. Table I summarizes the main parameters of these processes. Although Ge substitution is found to decrease the onset of the first crystallization process by 17 K, the second crystallization stage is shifted by 9 K to higher temperatures with respect to the Ge-free alloy. Therefore, whilst the amorphous state is thermally more stable for the Ge-free alloy, the nanocrystalline microstructure is more stable for the Ge-containing alloy.

Journal of Alloys and Compounds. Vol. 395. Núm. 1-2. 2005. Pag. 313-317
http://dx.doi.org/10.1016/j.jallcom.2004.11.057

3.2 Microstructure

As-cast samples of both studied alloys were heated up to the end of the first crystallization process, 873 K, to compare the nanocrystalline microstructures developed. The fully nanocrystallized state is interesting because it presents the maximum thermal stability against structural transformation, up to the onset of the second crystallization stage, and because some magnetic properties as the saturation magnetization are also maximized.

The XRD patterns of fully nanocrystallized samples (Figure 2) show for both alloys the (110) and (200) crystalline peaks corresponding to the α-Fe(Co) phase and an amorphous halo which overlaps with the (110) maximum. The lattice parameter of α-Fe was calculated from the position of the (110) and (200) peaks of this phase. A deconvolution procedure was applied to the (110) maximum of the α-Fe phase and the amorphous halo to obtain further information from the XRD patterns. After subtracting the background, the crystalline diffraction peak was fitted using a Lorentzian function, assuming the small grain size as the main effect of the peak broadening. The grain size was estimated from Scherrer formula. The amorphous halo was fitted using a Gaussian function. The crystalline volume fraction, *X*, was calculated from the ratio between the intensity area of the (110) maximum divided by the addition of this area plus the intensity area of the amorphous halo, *A*. This ratio was corrected taken into account the different average scattering power of the amorphous and crystalline phases [6]. The resulting parameters are listed in table II for the two studied alloys.

Although the lattice parameter of α-Fe is slightly higher for the Ge-containing than for the Ge-free alloy, the value of the former alloy could not correspond to a Ge content in the nanocrystals higher than 1-2 at. % [10]. Assuming that the distribution of Co throughout the nanocrystals and the amorphous matrix is homogeneous, as it was found for other nanocrystalline systems [11,12], the compositions of the nanocrystals might be close to $Fe_{95}Co_5$ for both studied

Journal of Alloys and Compounds. Vol. 395. Núm. 1-2. 2005. Pag. 313-317
http://dx.doi.org/10.1016/j.jallcom.2004.11.057
alloys, with possible presence up to ~2 at. % of Ge in the case of the alloy containing this element. Taking into account these compositions of the crystalline phase in the two studied alloys, their different B content yields a different correction factor for *A* to obtain *X*. This factor is 1 and 0.9 for the alloy with and without Ge, respectively. Therefore, both compositions develop similar nanocrystalline microstructure: *X* is very high at the end of the nanocrystallization, ~ 80 % and 70 % for the alloy with and without Ge, respectively. The estimated grain size is similar, although slightly smaller for the alloy without Ge (8 nm) compared to the alloy with Ge (11 nm).

3.3 Magnetic properties

Magnetic properties obtained at room temperature are summarized in table III for as-cast samples and those annealed at 873 K for 10 min of both studied compositions. Figure 3 shows the hysteresis loops of these samples. As it can be observed, the coercivity at the end of the nanocrystallization is similar to that of the as-cast state, ~10 A/m, one order of magnitude below the values observed in HITPERM alloys for a high crystalline volume fraction [1,6].

The saturation magnetization measured at room temperature increases after annealing for both samples, due to the formation of α-Fe(Co) crystallites. The value observed for the Ge-free alloy is similar to the maximum value achieved in FINEMET alloys [13], whereas the alloy with Ge shows a 10 % higher value of M_S.

In the framework of a detailed study of the variation of T_C^{am} on the annealing temperature, heating and cooling cycles at 10 K/min were performed in a Faraday magnetometer. Figure 4 shows the resulting curves from these *in situ* experiments. As cast samples were successively heated up to different annealing temperatures, T_A, and cooled down to 375 K, to see the effect on the Curie temperature and the thermal dependence of the saturation magnetization. Four annealing temperatures were chosen. Three of them were related to the peak temperature of the

Journal of Alloys and Compounds. Vol. 395. Núm. 1-2. 2005. Pag. 313-317
http://dx.doi.org/10.1016/j.jallcom.2004.11.057
first DSC exotherm, to perform equivalent thermal treatments: 67 K and 10 K below T_{p1} and 4 K above T_{p1}. The fourth annealing temperature was 873 K, which is considered to be the end of the nanocrystallization process. At this temperature, the sample was annealed for 10 min.

As-cast samples present a similar value of T_C^{am}, slightly higher for the Ge-free alloy. This value is ~200 K higher than that of previous studied nanocrystalline alloys with Ge [8]. The presence of Co in the compositions subject of this study is clearly effective enhancing the Curie temperature of the amorphous phase.

The first annealing temperature is enough below the onset of nanocrystallization to prevent the formation of nanocrystals, as it is evidenced by the presence of a paramagnetic regime extended from ~500 to ~750 K. Therefore, the observed effect is due to structural relaxation phenomena. For the other three thermal treatments, the magnetization progressively and irreversibly increases at temperatures above the onset.

After annealing 10 min at 873 K, it was not possible to detect the Curie temperature of the residual amorphous phase. It must be taken into account that at these high value of X the amorphous layer between the nanocrystals might be very thin (below 1 nm) and the ferromagnetic nanocrystals will polarize it. Therefore, the ferro-paramagnetic transition of the residual amorphous matrix will be smeared out and a large enhancement of the Curie temperature of this phase can be expected [14].

Figure 5 shows the values of T_C^{am} as a function of the annealing temperature. The dotted line divides the plot between amorphous and nanocrystalline samples. The structural relaxation phenomena do not affect the value of T_C^{am} of the Ge-free alloy but decrease by 6 K the value of T_C^{am} of Ge-containing alloy with respect to the as-cast sample. This behavior is different to that reported for FINEMET alloys, in which an increase of ~15 K of T_C^{am} was detected as a result of the structural relaxation [15]. Nanocrystallization yields in both cases to a continuous increase of

Journal of Alloys and Compounds. Vol. 395. Núm. 1-2. 2005. Pag. 313-317
http://dx.doi.org/10.1016/j.jallcom.2004.11.057
the Curie temperature of the amorphous matrix. It is worthy to note that, for similar annealing conditions, the alloy with Ge presents always a lower value of T_C^{am} than that of the alloy without Ge (~10 K). From this point of view, a partial substitution of Ge for B is not promising for an enhancement of the magnetic properties at high temperature. Although the partial substitution of Ge for Fe in NANOPERM alloys was proposed in this sense [8], it must be taken into account that both elements, Ge and B, are known to increase the Curie temperature of amorphous Fe-B alloys after partial substitution for Fe [16]. In this work, it is demonstrated that Ge does not produce an enhancement of T_C^{am} higher than B does.

However, there is a clear advantage of the partial substitution of Ge for B in the magnetic properties at high temperature. Figure 6 shows the M_S values as a function of the annealing temperature for different values of the temperature. As it can be observed, M_S of nanocrystallized samples is always higher in the Ge-containing alloy than in the Ge-free alloy, independently of the measuring temperature. As the nanocrystallization progresses, this difference increases up to ~10 %.

As it was said above, the maximum values of M_S observed at room temperature for FINEMET alloys are similar to that of the alloy without Ge and 10 % lower than that of the alloy with Ge. However, the high temperature response of M_S becomes better for the studied alloys than for FINEMET. As a comparison, in the temperature range from 573 to 773 K, M_S decreases ~ 45 % for nanocrystallized samples of FINEMET alloy [17], whereas M_S decreases only ~15 % in the case of the two alloys studied in this work. This effect is due to the presence of Si inside the crystalline phase of FINEMET alloys, which decreases the Curie temperature of the α-Fe phase down to ~850 K [18]. The estimated composition of the crystalline phase developed in the studied alloys, $Fe_{95}Co_5$, would present a Curie temperature ~1100 K, much higher than that of the nanocrystals of FINEMET alloys.

Journal of Alloys and Compounds. Vol. 395. Núm. 1-2. 2005. Pag. 313-317
http://dx.doi.org/10.1016/j.jallcom.2004.11.057

4. Conclusions

The present study on the effects of the partial substitution of Ge for B in nanocrystalline $Fe_{78}Co_5Zr_6B_{10}Cu_1$ yields the following conclusions:

- Partial substitution of Ge for B reduces, as expected, the onset of crystallization and increases the temperature of the second crystallization stage, increasing the thermal stability of the nanocrystalline microstructure. The microstructure at the end of the nanocrystallization is not seriously affected, although slightly larger grain size and higher crystalline volume fraction can be appreciated in the alloy with Ge.
- The room temperature coercivity of both studied compositions is ~10 A/m, one order of magnitude lower than that of HITPERM alloys. However, the Curie temperature of the amorphous phase is not enhanced by the partial substitution of Ge for B, although, the saturation magnetization increases about 10 % in the alloy with Ge with respect to the Ge-free alloy.

Acknowledgments

This work was partially supported by the Spanish Government and EU FEDER (Project MAT 2001-3175). J.S. Blázquez acknowledges a research contract from the Spanish Regional Government of Andalucía (Spain).

Journal of Alloys and Compounds. Vol. 395. Núm. 1-2. 2005. Pag. 313-317
http://dx.doi.org/10.1016/j.jallcom.2004.11.057

References

[1] M.E. McHenry, M.A. Willard, D.E. Laughlin, Progress in Mater. Sci. 44 (1999) 291.

[2] G. Herzer, IEEE Trans. Magn. 25 (1989) 3327.

[3] A. Hernando, M. Vázquez, T. Kulik, C. Prados, Phys. Rev. B 51 (1995) 3581.

[4] M.A. Willard, D.E. Laughlin, M.E. McHenry, D. Thoma, K. Sickafus, J.O. Cross, V.G. Harris, J. Appl. Phys. 84 (1998) 6773.

[5] J.S. Blázquez, V. Franco, A. Conde, M.R.J. Gibbs, H.A. Davies, Z.C. Wang, J. Magn. Magn. Mat. 250 (2002) 260.

[6] J.S. Blázquez, V. Franco, C.F. Conde, A. Conde, J. Magn. Magn. Mat. 254-255 (2003) 460.

[7] J.S. Blázquez, V. Franco, A. Conde, L.F. Kiss, J. Appl. Phys. 93 (2003) 2172.

[8] K. Suzuki, J.W. Cochrane, J.M. Cadogan, X.Y. Xiong, K. Hono, J. Appl. Phys. 91 (2002) 8417.

[9] R.C. O'Handley, *Modern Magnetic Materials: Principles and Applications*, (Wiley, New York, 1999) p. 227.

[10] W.B. Pearson, *A Handbook of Lattice Spacings and Structures of Metals and Alloys*, Vol 2 (Pergamon Press, Oxford, 1967) p. 911.

[11] Y. Zhang, J.S. Blázquez, A. Conde, P.J. Warren, A. Cerezo, Mater. Sci. Eng. A 353 (2003) 158.

[12] D.H. Ping, Y.Q. Wu, K. Hono, M.A. Willard, M.E. McHEnry, D.E. Laughlin, Scr. Mater. 45 (2001) 781.

[13] A. Lovas, L.F. Kiss, I. Balogh, J. Magn. Magn. Mat. 215-216 (2000) 463.

[14] A. Hernando, I. Navarro, C. Prados, D. García, F. Lesmes, J.J. Freijo, A. Salcedo, Nanostruct. Mater. 9 (1997) 459.

Journal of Alloys and Compounds. Vol. 395. Núm. 1-2. 2005. Pag. 313-317
http://dx.doi.org/10.1016/j.jallcom.2004.11.057

[15] J.S. Blázquez, S. Lozano-Pérez, A. Conde, Mat. Letters 45 (2000) 246.

[16] H.P.J. Wijn: In: Landolt-Börnstein: *Magnetische Eigenschaften von Metallen*, Vol. 19 (Springer Verlag, Berlin 1991) p. 93.

[17] M. LoBue, V. Basso, C. Beatrice, P. Tiberto, IEEE Trans. Magn. 36 (2000) 3035.

[18] C.F. Conde, M. Millán, A. Conde, J. Magn. Magn. Mat. 138 (1994) 314.

Journal of Alloys and Compounds. Vol. 395. Núm. 1-2. 2005. Pag. 313-317
http://dx.doi.org/10.1016/j.jallcom.2004.11.057

Figure captions

Figure 1. DSC scans at 10 K/min of the two studied alloys.

Figure 2. XRD pattern (CoKα) for samples heated at 10 K/min up to the end of the first crystallization process (873 K).

Figure 3. Hysteresis loops of as-cast samples and samples annealed 10 min at 873 K.

Figure 4. M_S signal of as-cast samples submitted to successive heating and cooling cycles. The long arrows indicate the right sense of the curve. The short arrows indicate the Curie temperature of the residual amorphous phase.

Figure 5. Curie temperature of the amorphous phase for samples previously heated up to different annealing temperatures. The dotted line divides the plot in amorphous (low temperatures) and nanocrystallized samples (high temperatures).

Figure 6. Saturation magnetization versus annealing temperature at different temperatures of measurement. The dotted line divides the plot in amorphous (low temperatures) and nanocrystallized samples (high temperatures).

Journal of Alloys and Compounds. Vol. 395. Núm. 1-2. 2005. Pag. 313-317
http://dx.doi.org/10.1016/j.jallcom.2004.11.057

Table I. Calorimetric results obtained at 10 K/min. T_x, onset temperature of crystallization; T_{pi}, peak temperature of the *i* process; H_i, enthalpy of the *i* process.

	$Fe_{78}Co_5Zr_6Cu_1B_5Ge_5$	$Fe_{78}Co_5Zr_6Cu_1B_{10}$
$T_x \pm 2$ K	749	766
$T_{p1} \pm 1$ K	773	790
$H_1 \pm 10$ J/g	85	93
$T_{p2} \pm 1$ K	1000	991
$H_2 \pm 5$ J/g	39	44

Journal of Alloys and Compounds. Vol. 395. Núm. 1-2. 2005. Pag. 313-317
http://dx.doi.org/10.1016/j.jallcom.2004.11.057

Table II. Microstructural parameters for samples heated up to the end of the nanocrystallization process, 873 K.

	$Fe_{78}Co_5Zr_6Cu_1B_5Ge_5$	$Fe_{78}Co_5Zr_6Cu_1B_{10}$
$D \pm 2$ nm	11	8
$X \pm 0.05$	0.81	0.72
$a \pm 0.0005$ nm	0.2871	0.2867

Journal of Alloys and Compounds. Vol. 395. Núm. 1-2. 2005. Pag. 313-317
http://dx.doi.org/10.1016/j.jallcom.2004.11.057

Table III. Room temperature magnetic properties of as-cast samples and samples heated up to the end of the nanocrystallization process, 873 K.

	$Fe_{78}Co_5Zr_6Cu_1B_5Ge_5$	$Fe_{78}Co_5Zr_6Cu_1B_{10}$
	As-cast (amorphous)	
$M_S \pm 5$ emu/g	127	110
$H_C \pm 2$ A/m	8	11
$T_C^{am} \pm 2$ K	515	523
	Heated up to 873 K (fully nanocrystallized)	
$M_S \pm 5$ emu/g	152	137
$H_C \pm 2$ A/m	8	7

Journal of Alloys and Compounds. Vol. 395. Núm. 1-2. 2005. Pag. 313-317
http://dx.doi.org/10.1016/j.jallcom.2004.11.057

Figure 1

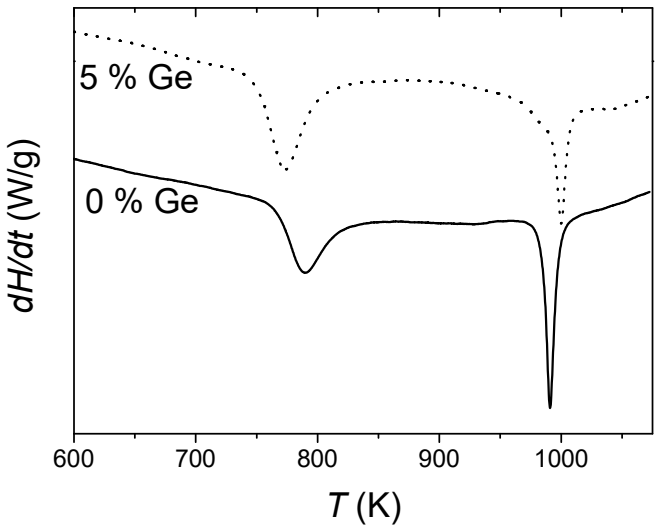

Journal of Alloys and Compounds. Vol. 395. Núm. 1-2. 2005. Pag. 313-317
http://dx.doi.org/10.1016/j.jallcom.2004.11.057

Figure 2

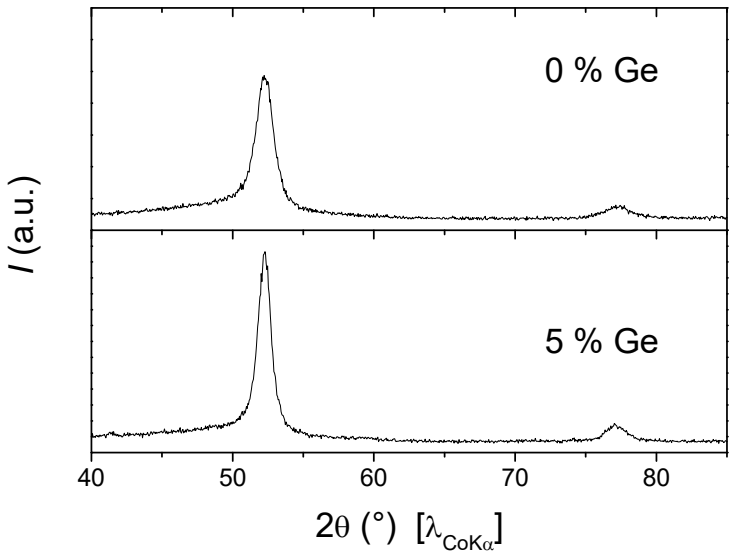

Journal of Alloys and Compounds. Vol. 395. Núm. 1-2. 2005. Pag. 313-317
http://dx.doi.org/10.1016/j.jallcom.2004.11.057

Figure 3

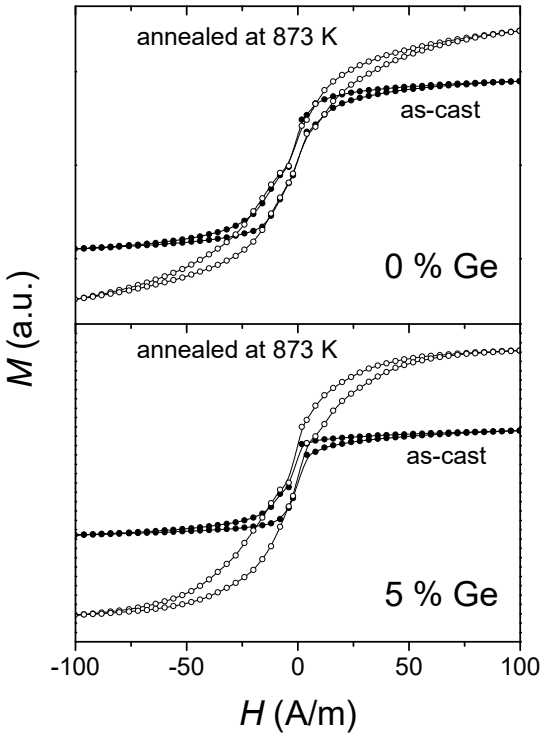

Journal of Alloys and Compounds. Vol. 395. Núm. 1-2. 2005. Pag. 313-317
http://dx.doi.org/10.1016/j.jallcom.2004.11.057

Figure 4

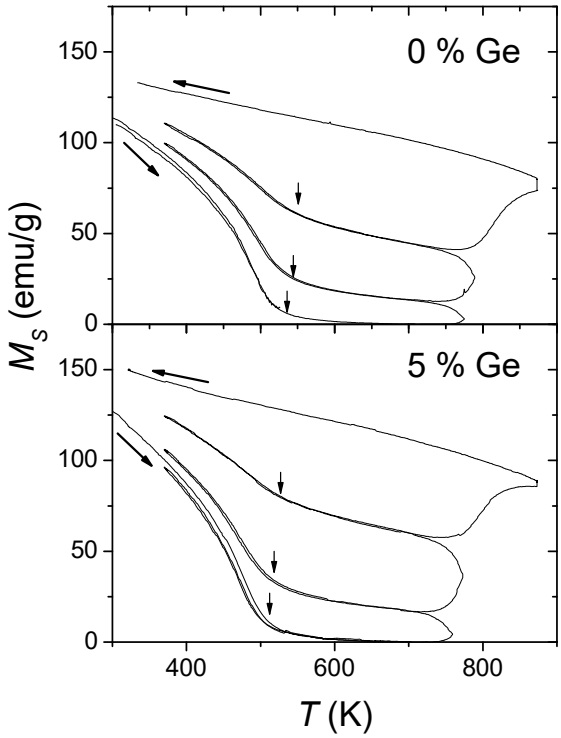

Journal of Alloys and Compounds. Vol. 395. Núm. 1-2. 2005. Pag. 313-317
http://dx.doi.org/10.1016/j.jallcom.2004.11.057

Figure 5

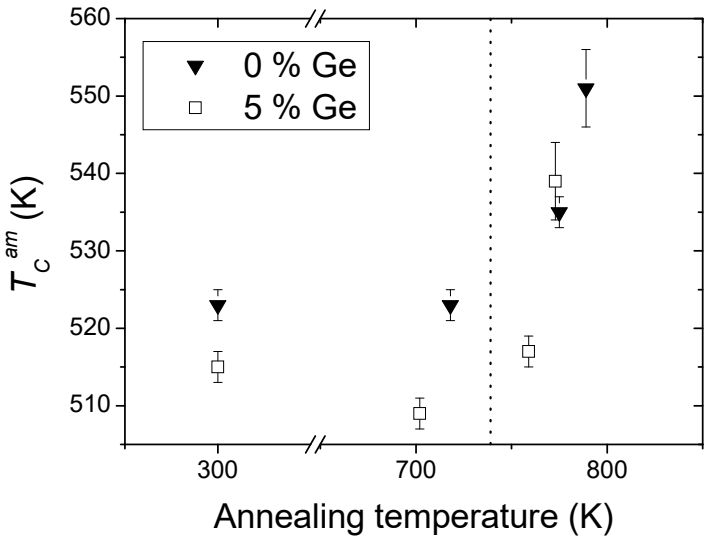

Journal of Alloys and Compounds. Vol. 395. Núm. 1-2. 2005. Pag. 313-317
http://dx.doi.org/10.1016/j.jallcom.2004.11.057

Figure 6